The Journal of Experimental Biology 215, 3242-3253

doi:10.1242/jeb.067942

RESEARCH ARTICLE

Ammonia excretion in the freshwater planarian *Schmidtea mediterranea*

Dirk Weihrauch[1,*], Ainsely C. Chan[1], Heiko Meyer[2], Carmen Döring[2], Mary Sourial[1] and Michael J. O'Donnell[3]

[1]Department of Biological Sciences, University of Manitoba, 190 Dysart Road, Winnipeg, MB, R3T 2N2, Canada, [2]Department of Zoology/Developmental Biology, University of Osnabrück, Barbarastrasse 11, Osnabrück, Germany and [3]Department of Biology, McMaster University, 1280 Main Street West, Hamilton, ON, L8S 4K1, Canada

*Author for correspondence (weihrauc@cc.umanitoba.ca)

SUMMARY

In aquatic invertebrates, metabolic nitrogenous waste is excreted predominately as ammonia. Very little is known, however, of the underlying mechanisms of ammonia excretion, particularly in freshwater species. Our results indicate that in the non-parasitic freshwater planarian *Schmidtea mediterranea*, ammonia excretion depends on acidification of the apical unstirred layer of the body surface and consequent ammonia trapping. Buffering of the environment to a pH of 7 or higher decreased the excretion rate. Inhibitor experiments suggested further that the excretion mechanism involves the participation of the V-type H^+-ATPase and carbonic anhydrase and possibly also the Na^+/K^+-ATPase and Na^+/H^+ exchangers. Alkalinization (pH 8.5, 2 days) of the environment led to a 1.9-fold increase in body ammonia levels and to a downregulation of V-ATPase (subunit A) and Rh-protein mRNA. Further, a 2 day exposure to non-lethal ammonia concentrations (1 mmol l^{-1}) caused a doubling of body ammonia levels and led to an increase in Rh-protein and Na^+/K^+-ATPase (α-subunit) mRNA expression levels. *In situ* hybridization studies indicated a strong mRNA expression of the Rh-protein in the epidermal epithelium. The ammonia excretion mechanism proposed for *S. mediterranea* reveals striking similarities to the current model suggested to function in the gills of freshwater fish.

Key words: ammonia trapping, Rh-protein, V-ATPase, high environmental ammonia, HEA.

Received 7 November 2011; Accepted 14 May 2012

INTRODUCTION

Ammonia is an end product of amino acid metabolism, but it can also be produced by ureolytic and uricolytic pathways. In this study, NH_3 refers to gaseous ammonia, NH_4^+ to ammonium ions and ammonia to the sum of both. Ammonia is a weak base (pK_a=9.2 to 9.8) and occurs in solutions in a pH-dependent equilibrium of uncharged, membrane-permeable NH_3 and ionic NH_4^+ (Cameron and Heisler, 1983). Although produced by essentially all cells, ammonia causes a number of toxic effects in animal systems.

Likely most severe are the effects of ammonia on the central nervous system, as reported extensively for mammalian systems. Here ammonia causes swelling and cell death of astrocytes (Butterworth, 2002; Ip and Chew, 2010) and excessive activation of *N*-methyl-D-aspartate (NMDA)-type glutamate receptors (Marcaida et al., 1992). Ammonia has a further direct inhibitory effect on the astrocytic EAAT-1 (GLAST) and EAAT-2 (GLT-1) transporters, which are responsible for the removal of glutamate from the neuronal synapse (Chan et al., 2000; Knecht et al., 1997; Norenberg et al., 1997). Very high mRNA expression levels of Rhesus (Rh)-like ammonia transporters observed in the ganglia of the tobacco hornworm, *Manduca sexta* (Weihrauch, 2006), and the fruit fly *Drosophila melanogaster* (FlyAtlas, http://flyatlas.org) (Chintapalli et al., 2007) suggest that cells in the central nervous system of invertebrates also require a capacity to transport ammonia.

Because of its toxic effects, ammonia must be rapidly excreted or metabolized to less toxic substances to keep its concentration in the body fluids within a tolerable range. With the exception of mammals and elasmobranchs, the vast majority of aquatic living species, including fully aquatic amphibians (Cragg et al., 1961; Fanelli and Goldstein, 1964; Wood et al., 1989), teleost fish (Weihrauch et al., 2009; Wright and Wood, 2009) and virtually all aquatic invertebrates (Wright, 1995), are ammonotelic, excreting the majority of their nitrogenous waste directly as ammonia.

Excretion usually occurs across gas-exchanging or ionoregulatory epithelia, such as the gills (Potts, 1965; Weihrauch et al., 2004b; Weihrauch et al., 2009; Wilson et al., 1994; Wright and Wood, 2009), the anal papillae (Donini and O'Donnell, 2005) or the skin (Fanelli and Goldstein, 1964; Shih et al., 2008). However, very little is known about the actual excretion mechanisms. With the discovery by Marini and coworkers that members of the Rh family function as ammonia transporters (Marini et al., 2000), this field of research gained considerable momentum over the last decade. The majority of studies focusing on ammonia excretion mechanisms in aquatic species were performed on decapod crustaceans and fish, as reviewed by Weihrauch and coworkers for crustaceans (Weihrauch et al., 2004b; Weihrauch et al., 2009) and by Wright and Wood for fish (Wright and Wood, 2009).

In crustaceans such as the green shore crab, *Carcinus maenas*, branchial ammonia excretion is an active process, involving the basolateral Na^+/K^+-ATPase, an intracellular (vesicular) H^+-ATPase (V-ATPase), a functional microtubule system and likely also Rh-like ammonia transporters and apical cation/H^+ exchangers (Lucu et al., 1989; Martin et al., 2011; Weihrauch et al., 1998; Weihrauch et al., 2004b; Weihrauch et al., 2002).

In contrast to the ammonia excretion modus in brackish-water and marine crabs, branchial ammonia excretion in freshwater fish

depends on an acidification of the unstirred boundary layer on the apical surface of the gill (Weihrauch et al., 1998; Wilson et al., 1994). Ammonia from the blood appears to enter the pavement cell cytoplasm *via* the Na^+/K^+-ATPase and a basolateral isoform of the Rh-like ammonia transporter, Rhbg. It is further proposed that an apical V-ATPase, perhaps in concert with the Na^+/H^+ exchanger NHE2, causes a local acidification of the gill boundary layer, thereby lowering the partial pressure of NH_3 (P_{NH_3}). The resulting partial pressure gradient of ammonia (ΔP_{NH_3}) across the apical membrane thus drives cellular NH_3 into the environment *via* a second Rh-protein, Rhcg2. Protons to fuel the V-ATPase/NHE are provided by the activity of an intracellular carbonic anhydrase (Nawata et al., 2007; Nawata and Wood, 2008; Nawata and Wood, 2009; Nawata et al., 2010b).

Mechanistic studies on ammonia excretion mechanisms in aquatic invertebrates other than crustaceans are very sparse. The present study provides the first insights into the ammonia excretion mechanisms in *Schmidtea mediterranea*. This carnivorous freshwater planarian of the phylum Platyhelminthes has recently become an important model system for the investigation of regeneration and stem cell biology (Sánchez Alvarado and Tsonis, 2006), but very little is known about its physiology. The epidermis of the planarian consists of a monostratified epithelium, which is multiciliated on the ventral side. Mucus-secreting gland cells (rhabdites) are located between the epithelial cells of the epidermis (Rompolas et al., 2009; Stevenson and Beane, 2010). Excretion experiments, together with gene expression analysis and *in situ* hybridization studies, provide the first evidence that a freshwater invertebrate organism excretes ammonia *via* the epidermis in a manner similar to that proposed for branchial excretion in freshwater fish.

MATERIALS AND METHODS

Animals

Schmidtea mediterranea Benazzi, Baguñà, Ballester, Puccinelli & Del Papa 1975 were kept at room temperature under natural light settings in ca. 6 litre dechlorinated tap water per gram fresh mass (FM). Water was aerated by means of an air stone and animals were fed once per week with small pieces of bovine liver. After feeding, the tank water was replaced. Ammonia levels in the tanks were monitored on a regular basis and varied between 3 and 15 $\mu mol\,l^{-1}$ total ammonia. All animals were starved for 2 days before experimentation. All experiments were performed at room temperature during daylight.

Whole-body excretion experiments

For all whole-body excretion experiments, a number of animals (ca. 0.1–0.15 g FM, ≥0.5 cm in length) were transferred into small glass containers (diameter=2.5 cm, depth=2 cm) filled with 4 ml of dechlorinated tap water. After an equilibration period of 0.5 h, the water was replaced with 4 ml of fresh water for the first sampling period. Each sampling period lasted 1 h. At the end of each sampling period, two samples of 1.9 ml were taken from the container for later analysis of water ammonia. Before each experimental step, animals were rinsed by adding and draining 8 ml of dechlorinated tap water into and from the container, respectively.

Feeding experiments

In another series of experiments, a feeding period (bovine liver, *ad libitum*) of 1 h followed the control measurement (see above). To avoid stressful animal transfer, feeding took place in the experimental container, filled with 8 ml water. After a rinse of the experimental container with 8 ml of dechlorinated tap water, 4 ml of dechlorinated ammonia-free tap water was added (see above) and the first sampling period after feeding followed, which lasted for 1 h. Four consecutive 1-h sampling periods followed, including a washing step. After these five consecutive 1-h sampling periods in ammonia-free water, the glass containers, which contained a pool of individual animals (total mass=0.15–0.25 g), were covered with a plastic mesh and were then placed into a 6 liter tank of dechlorinated tap water (aerated and ventilated by several air stones) until the final measurement took place 16 h after feeding. The mesh allowed free water exchange but not the passage of the animals. Samples were sealed and immediately frozen at –80°C for later analysis of total ammonia, usually within 1 week.

Excretion experiments in various pH regimes

In experiments to determine excretion rates in pH-buffered media, a control sampling period in dechlorinated, non-buffered tap water (1 h, pH 8.3) was followed by a rinse and one experimental sampling period (1 h) employing water buffered to one particular pH with either 10 $mmol\,l^{-1}$ 2-(*N*-morpholino)ethanesulfonic acid (MES; for a pH of 5, 5.5 or 6), HEPES (for a pH of 6.5, 7 or 7.5) or 2-amino-2-hydroxymethyl-propane-1,3-diol (Tris base; for a pH of 8 and 8.5). Final concentrations of experimental solutions were adjusted with HCl or NaOH to the experimental pH.

Excretion experiments under the influence of varying inhibitors and after short-term exposure to various ammonia concentrations

In experiments to determine excretion rates under the influence of an inhibitor, a control sampling period employing dechlorinated, non-buffered tap water (1 h, pH 8.3) was followed by a rinse and a 30 min pre-incubation period in media containing the inhibitor. A rinse was followed by a 1 h experimental sampling period. Inhibitors were purchased from Sigma-Aldrich (St Louis, MO, USA) and were prepared, with the exception of colchicine, at a concentration range known to be effective in other invertebrates (Blaesse et al., 2010; Onken and McNamara, 2002; Weihrauch et al., 2004a). The concentrations were: 5 $\mu mol\,l^{-1}$ concanamycin C, 1 $mmol\,l^{-1}$ acetazolamide, 10 $mmol\,l^{-1}$ amiloride hydrochloride hydrate, 1 $mmol\,l^{-1}$ ouabain and 10 $mmol\,l^{-1}$ colchicine. Amiloride hydrochloride hydrate and concanamycin C were dissolved in dimethyl sulfoxide (DMSO) at a final concentration of 0.5%. In these experiments, 0.5% DMSO was also added to the control solutions.

In a series of experiments, animals were exposed after an initial control sampling period to different environmental ammonia concentrations (0.1, 0.2, 0.5, 1, 5 and 10 $mmol\,l^{-1}$ NH_4Cl; $N \geq 5$ for all treatments) for 1 h. After this short-term ammonia exposure, ammonia excretion rates were measured in ammonia-free water consecutively over a period of 4 h.

At the end of each experiment, animals were dried between paper towels, weighed and placed in a separate tank for a monitoring period of 7 days. The collected samples were only used for analysis if the animals survived the monitoring period after any given treatment. The samples were analyzed for their content of total ammonia on the day of experimentation or were sealed and immediately frozen at –80°C for later analysis, usually within 1 week.

Long-term pH and high environmental ammonia exposure experiments

For long-term exposure experiments, groups of animals (ca. 1 g FM in 2 litres dechlorinated tap water) were kept for 48 h either in a

particular concentration of NH_4Cl (0.1, 0.2, 0.5, 1, 5, 10 mmol l^{-1}, not buffered, adjusted to pH 8.3) or in dechlorinated tap water buffered with 10 mmol l^{-1} MES (pH 5.5), HEPES (pH 7) or Tris base (pH 8.5). Experimental solutions were adjusted with HCl or NaOH to the experimental pH. After 24 h the experimental solutions were refreshed. Tissue collection for analysis followed after a total exposure time of 48 h.

Ammonia concentration of animal tissue

For measurements of whole-body ammonia concentration, animals were carefully dried between paper towels and weighed. A pool of animals from a certain treatment with a total FM of approximately 0.1 g was placed in 1 ml of deionized water and homogenized on ice for 15 s using a polytron homogenizer (AHS, Pro Scientific, Oxford, CT, USA). Immediately after homogenization, the pH of the homogenate was determined followed by an addition of 3 ml of ice-cold deionized water enriched with 5 mmol l^{-1} Na^+-azide to avoid ammonia production from remaining microorganisms (Downie et al., 1979). After centrifugation (5000 ***g***, 5 min, 4°C) the ammonia concentration of the supernatant was determined (see below). Because of possible proteolytic ammonia generation during the homogenization process, a slight error towards higher values in total body ammonia concentration cannot be excluded.

Ammonia measurement

The concentration of total ammonia was measured in magnetically stirred samples using a gas-sensitive NH_3 electrode (Thermo Orion, Beverly, MA, USA) connected to a pH meter. For a detailed description of the method, refer to Weihrauch et al. (Weihrauch et al., 1998). Ammonia sensitivity of the electrode was high and amounted to ±1.5 μmol l^{-1} total ammonia in the concentration range of 50 to 200 μmol l^{-1} and ±1 μmol l^{-1} total ammonia in the concentration range of 4 to 50 μmol l^{-1}. All standard curves were prepared using the corresponding experimental solutions.

Immunohistochemistry and western blotting

Immunostaining was carried out essentially as described in Sánchez Alvarado and Newmark (Sánchez Alvarado and Newmark, 1999). In brief, whole animals were first treated with 2% HCl in H_2O for 5 min and fixed in Carnoy's fixative for 2 h. After 1 h in 100% methanol, they were bleached with a cold lamp in 6% H_2O_2/methanol for 16 to 20 h at room temperature without shaking. Animals were then rehydrated by a series of methanol/PBSTx (phosphate buffered saline supplemented with 0.3% Triton X-100) washes (75, 50 and 25%) for 10 min each at room temperature. After two washes in 100% PBSTx, animals were blocked for 2 h in 1% Rotiblock (Carl Roth, Karlsruhe, Germany)/PBSTx (blocking buffer) at room temperature. Subsequently, animals were incubated with primary antibodies [V-ATPase subunit B specific, raised in guinea pig against *M. sexta* antigen, diluted 1:100 (Weng et al., 2003)] for 20 h at 4°C in blocking buffer. The negative control was incubated in parallel in the same buffer without the addition of antibodies. Eight washes in PBSTx (1 h each) were followed by 1 h in blocking buffer with all steps performed at room temperature. The secondary antibody (Cy3-conjugated anti guinea pig, Jackson ImmunoResearch, Newmarket, Suffolk, UK) was diluted 1:200 in blocking buffer and positive and negative samples were incubated for 14–16 h at 4°C. Finally, animals were washed for 3–4 h in PBSTx at room temperature.

For cryosections (10 μm), stained specimens were subjected to an increasing sucrose gradient (10, 20 and 30% in PBS) prior to embedding them in tissue freezing medium (Jung, Nussloch, Germany). Freezing was conducted in isopentane cooled in liquid nitrogen. Subsequent to sectioning (Leica CM1900 cryomicrotome, Leica Microsystems, Wetzlar, Germany), frozen tissues were transferred to glass slides (superfrost, Microm International, Walldorf, Germany), fixed by short-term warming (10 s, 50°C), washed three times (PBS, 5 min each) and embedded in VectaShield (Vector Laboratories, Burlingame, CA, USA). Sections were visualized using either a stereomicroscope (Leica MZ16 FA) or a confocal laser scanning microscope (LSM 5 Pascal, Carl Zeiss Microscopy, Göttingen, Germany).

Western blotting was carried out essentially as previously described (Meyer et al., 2009). Briefly, animals were homogenized (glass-Teflon homogenizer) in PBS containing protease inhibitor mix M (Serva, Heidelberg, Germany). Subsequently, Laemmli buffer was added and samples were boiled at 99°C for 3 min. Protein samples (15 μg lane^{-1}) were separated by SDS-PAGE and transferred to nitrocellulose membranes. The primary antibody (anti V-ATPase subunit B) was applied at a dilution of 1:1000 and visualized by anti-guinea pig alkaline phosphatase conjugated antibody (1:10,000, Sigma-Aldrich).

In situ hybridization and riboprobe synthesis

Whole-mount *in situ* hybridization was carried out as previously described (Umesono et al., 1999) including a triethanolamine treatment as described in Nogi and Levin (Nogi and Levin, 2005). Proteinase K (20 μg ml^{-1}) treatment was performed for 8 min at 37°C. The DIG-labelled riboprobes were used at 0.2 ng μl^{-1} for hybridization, which was performed at 55°C for 60 h. Primers used for synthesis of the probes for Rh-like protein were (5′→3′) atgattcaaccatggggtgca (forward) and ttaaaacttttttcatttcgat (reverse), resulting in an amplicon of 486 bp. Subsequently, the respective sequence was cloned into the pGEM-T easy vector system (Promega, Madison, WI, USA) and sense as well as antisense riboprobes were synthesized with the DIG RNA labelling kit according to the manufacturer's instructions (Roche, Mannheim, Germany).

Quantitative real-time PCR

For total RNA isolation, animals with a combined FM of approximately 0.1 g were homogenized in TRIzol reagent (Invitrogen, Carlsbad, CA, USA), employing a polytron homogenizer that was pre-treated with RNase AWAY (Invitrogen). Following DNase treatment (DNase 1, Invitrogen), RNA was tested for purity by a high-cycle PCR using the primer pair actin F1/actin R1 (Table 1) targeting cytoplasmic actin (GenBank accession no. EG415476). For cDNA synthesis, 1 μg of DNA-free total RNA (showing no PCR products) was reversely transcribed using oligo (dT) primers and *Thermoscript* reverse transcriptase (Invitrogen).

The quality of cDNAs generated from all tissues was assessed by PCR employing the primer pair actin F1/actin R1. All PCR products were evaluated by gel electrophoresis, ethidium bromide staining and UV visualization. Primers to be employed in quantitative PCR targeting the Rh-like protein, V-ATPase (subunit A) and Na^+/K^+-ATPase (α-subunit) were designed based on published sequences (GenBank accession nos EG404114, EG416580 and EG346594, respectively) and showed a single band of the predicted size after PCR and gel visualization (Table 1). Sequencing of the purified PCR products (QIAquick Gel Extraction Kit, Qiagen, Mississauga, ON, Canada) confirmed the correctness of the amplicon. For quantitative PCR (Miniopticon, Biorad, Mississauga, ON, Canada), standard curves were generated using a dilution series with quantities of 10^{-2}, 10^{-3}, 10^{-4}, 10^{-5}, 10^{-6} and 10^{-7} ng DNA of the respective purified PCR product of the target

Table 1. Primers employed in real-time PCR targeting Rhesus (Rh)-like ammonia transporter, V-type H^+-ATPase (subunit A), Na^+/K^+-ATPase (α-subunit) and actin from *Schmidtea mediterranea*

Primer	Nucleotide sequence (5′→3′)	Annealing temperature (°C)	Product size (bp)
Rh-protein			
RhF2	GGTATGCCTGGTATCATGGG	60	285
RhR2	CGTCTCTTCTGAAACGGTCCA	60	
V-ATPase			
HAT F1	ACCTTAGAAGTGGCCCGTTT	60	211
HAT R1	TGGTATCACCCATTGCTTCA	60	
Na^+/K^+-ATPase			
NaK F1	TCAGGAATGGGGATTCAGAC	60	261
NaK R1	GGTAGCCACCACGTGAATCT	60	
Actin			
Actin F1	TTGGCCGGTAGAGATTTGAC	55	156
Actin R1	AGCTGCAGTTGCCATTTCTT	55	

gene. A minimum R^2 value of 0.98 for the standard curve was required. Real-time PCR assays were performed employing SsoFast EvaGreen supermix (Biorad) in a 15 µl assay. After 40 cycles, the quality of all PCR products was evaluated by performing a melting curve analysis as well as gel electrophoresis and ethidium bromide/UV visualization.

Chemicals

Unless stated otherwise, all chemicals were purchased from Sigma-Aldrich.

Statistics

Values are reported as means ± s.e.m. Statistical tests performed included Student's *t*-tests for comparing two means and one-way ANOVA for comparing more than two means. *P*-values ≤0.05 were considered statistically significant. The statistical method employed in each particular experiment is given in the respective figure legends.

RESULTS

Ammonia excretion and feeding

Under control conditions, *S. mediterranea* excreted 0.70±0.03 µmol g^{-1} FM h^{-1} ammonia (*N*=48) and the whole-body ammonia concentration was 1.9±0.1 µmol g^{-1} FM (*N*=6; data not shown). Feeding increased excretion rates significantly. One hour after feeding, ammonia excretion rates increased ca. fourfold and reached a maximum 3 h after feeding. Ammonia excretion rates declined slightly over time, but remained approximately threefold above the unfed controls 16 h after feeding (Fig. 1). One hour after ammonia excretion rates reached their maximum, relative mRNA expression levels of the Rh-protein and the V-ATPase (subunit A) were determined. At this time relative mRNA expression levels of the Rh-protein (*N*≥3) were elevated (*P*<0.038, one-tailed *t*-test). There was also a small but significant increase in the mRNA expression level of the V-ATPase (subunit A) (*N*=4; Fig. 2). The internal control used in all mRNA expression experiments was actin, which showed no difference in absolute mRNA expression levels after *S. mediterranea* was subjected to different treatments (*N*≥4), including a 2 day exposure to varying pH regimes and elevated ammonia concentrations (data not shown).

Short-term exposure to high environmental ammonia

As seen in Fig. 3, short-term exposure to 0.1 and 0.2 mmol l^{-1} NH_4Cl had no effect of the excretion rates following high environmental ammonia (HEA) exposure. Short-term exposure to 0.5, 1, 5 and 10 mmol l^{-1} NH_4Cl caused an increase in the excretion rate in the hour following the exposure, which decreased rapidly in the second hour after the treatment to control levels for 0.5 and 1 mmol l^{-1} NH_4Cl exposures and to near-control levels for 5 and 10 mmol l^{-1} NH_4Cl exposures. Control levels were reached in the third hour after 10 mmol l^{-1} HEA exposure.

Ammonia excretion mechanism

Ammonia excretion in *S. mediterranea* depended on the acidification of the apical unstirred boundary layer of the epidermis. In comparison to excretion rates recorded in unbuffered freshwater (control, pH 8.3), higher and lower values were found in media buffered to pH 5 and above pH 7, respectively. In media buffered to a pH of 5.5, 6.0 and 6.5, ammonia excretion rates did not differ from rates measured under control conditions. Fig. 4 shows excretion rates as a percentage of the respective controls (*N*=6 for all treatments).

Inhibition of V-ATPase by addition of 5 µmol l^{-1} concanamycin C to the environmental solution reduced the ammonia excretion rate by 49.2±5.4% (*N*=6). A similar reduction in the excretion rate was found after blockage of apical NHEs and/or Na^+ channels employing 10 mmol l^{-1} amiloride hydrochloride hydrate (*N*=6) or inhibiting the Na^+/K^+-ATPase by 1 mmol l^{-1} ouabain (*N*=4). Moreover, a concentration of 1 mmol l^{-1} acetazolamide, an inhibitor of the carbonic anhydrase, reduced the ammonia excretion rate by 37.8±2.4% (*N*=6). Disrupting the microtubule network by 10 mmol l^{-1} colchicine (*N*=6) did not have a significant effect on the excretion rate (Fig. 5). Application of 2 mmol l^{-1} amiloride hydrochloride hydrate had no effect on the excretion rate (*N*=6, data not shown).

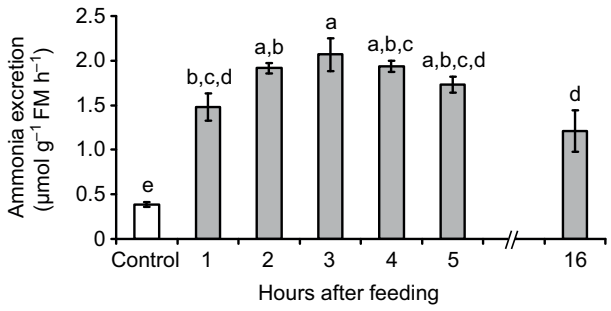

Fig. 1. Ammonia excretion rates (means ± s.e.m.) of *Schmidtea mediterranea* before (control) and after a feeding period of 1 h (*N*=6). Significant differences are indicated by different letters. Data were analyzed employing a one-way ANOVA with repeated measures using a Tukey's pairwise comparison.

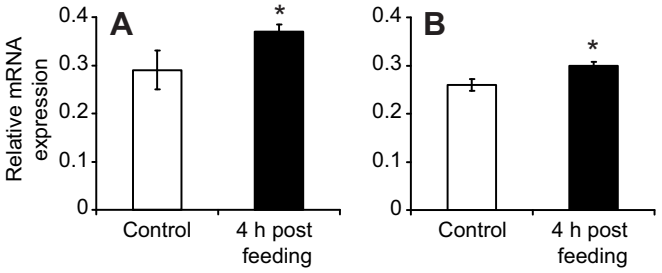

Fig. 2. Relative mRNA expression levels (means ± s.e.m.) of (A) Rh-like protein (N=3) and (B) V-ATPase (subunit A) (N=4) in *S. mediterranea* before and 4 h after feeding. The ratio of absolute expression levels of the target genes and actin is shown. Asterisks indicate significant differences between treatments. Data were analyzed employing a one-tailed Student's *t*-test.

A monitoring period of 1 week following each experiment revealed that none of the treatments caused any mortality (data not shown). The inhibitory effect of acetazolamide (1 mmol l^{-1}) on the ammonia excretion rate was counteracted by lowering the medium pH from 8.3 (control) to 5 (buffered with MES) (N=4; Fig. 6).

As shown in Fig. 7A, in *S. mediterranea* protein extracts (whole animals), the V-ATPase antiserum detected a dominant protein band with a molecular mass of approximately 56 kDa, which corresponds to the molecular masses already calculated for B-subunits from other invertebrate species (Merzendorfer et al., 1997; Weihrauch et al., 2001). The distinct detection of this band is considered as strong indication for the presence of a V-ATPase in this organism, with its subunit B being recognized rather specifically by the applied antiserum.

Immunohistochemical analyses of *S. mediterranea* cross-sections using the same antiserum detected the V-ATPase (subunit B) in the epidermis of the animal (Fig. 7B,C,D,F,G) with an apparent accumulation in rod-shaped structures, presumably rhabdites (Fig. 7B,F,G, arrows).

To analyze the expression pattern of the Rh-like ammonia transporter (GenBank accession no. DN307511) and to relate this pattern to V-ATPase expression, we generated riboprobes specific to the corresponding mRNA and used them for *in situ* hybridizations. As depicted in Fig. 8, mRNA coding for the Rh-like protein was detected predominately in the epidermis. In control animals incubated with sense probes no staining was visible.

The effect of environmental pH

A 2 day exposure to strongly buffered medium adjusted to a pH of 8.5 caused a nearly twofold increase of the whole-body ammonia concentration from 1.95±0.5 µmol g^{-1} FM (N=4) to 3.58±0.4 µmol g^{-1} FM (N=6), whereas exposure to media buffered to pH 5.5 (N=4) and pH 7 (N=5) caused a slight but significant decrease (Fig. 9). In all applied external pH regimes (non-buffered freshwater, N=6; pH 5.5, N=4; pH 7, N=4; and pH 8.5, N=6), the body pH remained unaltered at 7.18±0.06 (data not shown).

The relative mRNA expression levels for both the Rh-protein and the A subunit of the V-ATPase were correlated to medium pH (N≥4). Compared with controls (non-buffered medium, pH 8.3) the low pH and high pH buffered media caused an upregulation and downregulation of the Rh-protein, respectively, whereas a similar expression level was measured in animals exposed for 2 days to pH 7. Relative expression levels of the V-ATPase (subunit A) in animals exposed to pH 5.5 and 7 were upregulated when compared with controls, whereas in animals exposed to pH 8.5 the V-ATPase showed a trend towards downregulation (Fig. 10).

Long-term exposure to HEA

Long-term exposure to 5 and 10 mmol l^{-1} NH_4Cl was lethal to *S. mediterranea*, causing death after 48 and 24 h, respectively (N=6).

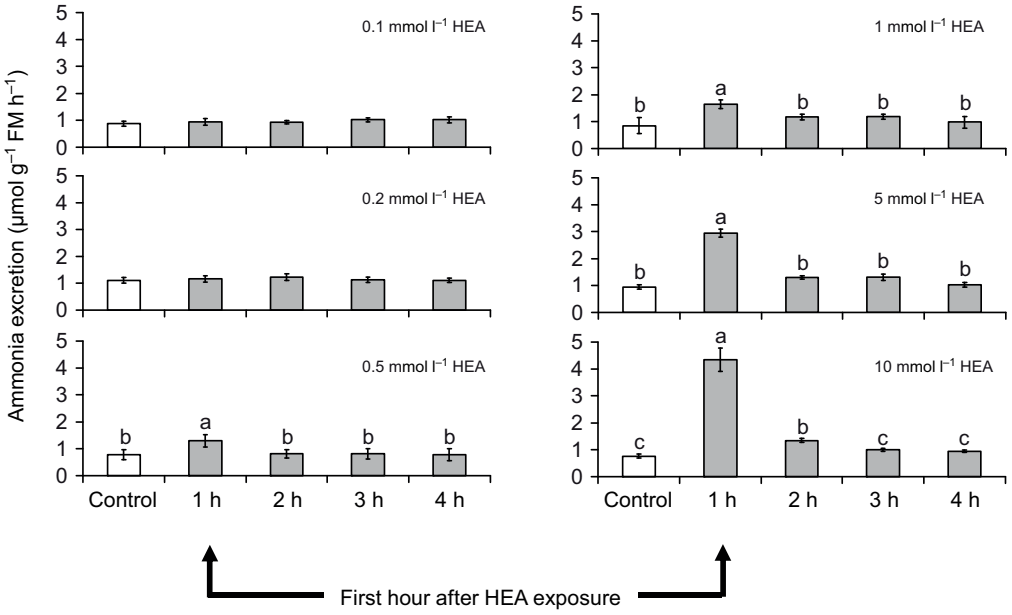

Fig. 3. Ammonia excretion rates (means ± s.e.m.) of *S. mediterranea* before (control) and after short-term exposure (1 h) to different high environmental ammonia (HEA) concentrations (0.1, 0.2, 0.5, 1, 5 and 10 mmol l^{-1} NH_4Cl; N=6 for all treatments). Ammonia excretion rates of four consecutive hours after feeding are shown; the first hour after HEA exposure is indicated. Significant differences are indicated by different letters. Data were analyzed employing a one-way ANOVA with repeated measures using a Tukey's pairwise comparison.

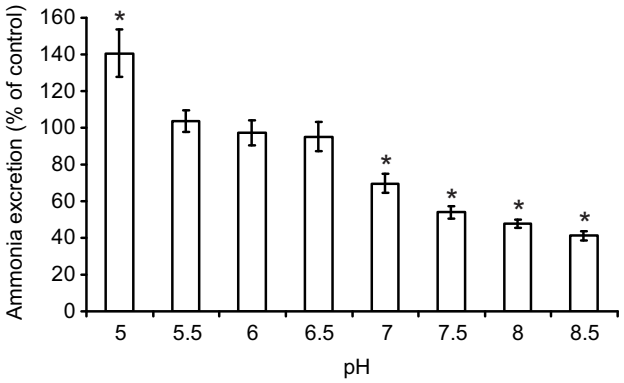

Fig. 4. Ammonia excretion of *S. mediterranea* in media adjusted and buffered to various pH regimes. The values represented indicate the percentage of the control (dechlorinated tap water, pH 8.3; means ± s.e.m., *N*=6 for all pH regimes). Asterisks indicate significant differences from the control value. Data were analyzed statistically employing a paired Student's *t*-test (two-tailed) on the original excretion rate values.

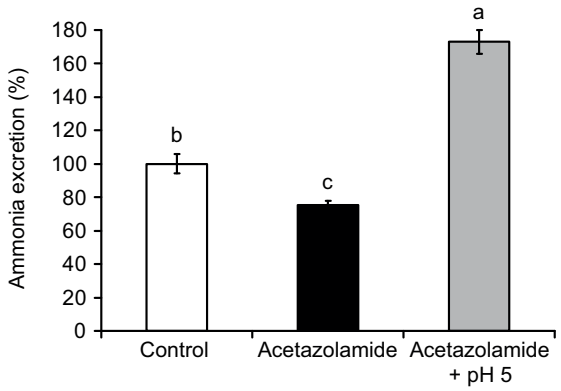

Fig. 6. Effect of acetazolamide and low pH (pH 5.5, 10 mmol l^{-1} MES) on ammonia excretion rates (means ± s.e.m.) in *S. mediterranea*. Values are given as percentage of values measured without addition of any inhibitor (*N*=4). Data were analyzed on the non-transformed values employing a one-way ANOVA with repeated measures using a Tukey's pairwise comparison.

Exposure of up to 1 mmol l^{-1} NH_4Cl was tolerated by *S. mediterranea* for an extended time period of at least 1 week. After 48 h of exposure to 0.1, 0.2, 0.5 and 1 mmol l^{-1} NH_4Cl, body ammonia concentrations increased with increasing environmental ammonia concentrations (*N*=5; Fig. 11).

HEA also led to an increase in mRNA expression levels of the Rh-protein (0.5 and 1 mmol l^{-1} NH_4Cl; *N*=4) and the Na^+/K^+-ATPase (α-subunit) (1 mmol l^{-1} NH_4Cl; *N*=4), but had no effect on relative mRNA expression levels of the V-ATPase (subunit A) (*N*=4; Fig. 12).

DISCUSSION

Ammonia excretion rates measured in *S. mediterranea* fell within the range measured for other freshwater organisms. As a comparison, excretion rates for rainbow trout (*Oncorhynchus mykiss*) and *Xenopus laevis* tadpoles amount to ca. 0.4 and 0.64 μmol g^{-1} FM h^{-1}, respectively (Wildling and Kerschbaum, 2007; Zimmer et al., 2010). Rates for developing zebrafish larvae (9 days post fertilization) are ca. 2 μmol g^{-1} FM h^{-1} (Braun et al., 2009).

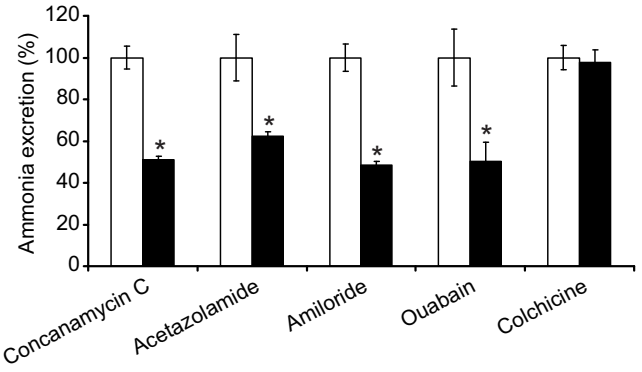

Fig. 5. Effects of different inhibitors on ammonia excretion rates (means ± s.e.m.) in *S. mediterranea*. Control values for each treatment were set to 100% (open bars), with values measured under the influence of the inhibitors given as percent of the respective control (filled bars). The concentrations of the inhibitors were: 5 μmol l^{-1} concanamycin C (*N*=6), 1 mmol l^{-1} acetazolamide (*N*=6), 10 mmol l^{-1} amiloride (*N*=6), 1 mmol l^{-1} ouabain (*N*=4) and 10 mmol l^{-1} colchicine (*N*=6). Asterisks indicate significant differences from the control value. Data were analyzed employing a paired Student's *t*-test (two-tailed) on excretion rates prior to calculation of percentage values.

Immediately after feeding, ammonia excretion rates roughly quadrupled compared with controls (Fig. 1), an increase in metabolic ammonia production similar to that observed in the green shore crab, *C. maenas* (Weihrauch, 1999), but much higher than values in rainbow trout (Zimmer et al., 2010), where excretion rates increase not directly after food intake but after a delay of approximately 2 to 4 h. Feeding also leads to subsequent increases in mRNA expression levels of branchial Rhcg2 and the V-ATPases (subunit B) in trout (Zimmer et al., 2010). In the flatworm, the degree of increase of mRNA expression levels of the Rh-protein and the V-ATPases (subunit A) was comparatively low. However, here it is important to note that *S. mediterranea* RNA was isolated from whole animals and not from a particular ammonia-excreting tissue. Changes in expression levels of the Rh-protein and the V-ATPase may thus be greater in the epidermis or other potential ammonia transporting tissues after treatments such as feeding. For *S. mediterranea* it is assumed that an upregulation of the Rh-protein and the V-ATPase would promote ammonia excretion, when elevated excretion rates are necessary to maintain body fluid ammonia levels in a tolerable range. Unfortunately, in this study direct measurements of pH and ammonia concentrations in the interstitial fluid were not possible, so we could not put these parameters into perspective with excretion rates and changes in gene expression levels.

For an indirect estimation of the interstitial fluid ammonia levels and the capacity to maintain these ammonia levels within the body fluids, animals were exposed to a variety of different environmental ammonia concentrations for short periods and post-exposure excretion rates were monitored (Fig. 3). After exposure to 0.1 and 0.2 mmol l^{-1} NH_4Cl, ammonia excretion rates did not differ from control rates, suggesting that during this short-term exposure no ammonia was accumulated within the body fluids and ammonia excretion continued uncompromised. Consequently, the animals either possess an active or secondary active ammonia excretion mechanism, which functions when interstitial fluid levels are equal or below 0.2 mmol l^{-1}, as seen in the hemolymph of decapod crabs (Martin et al., 2011; Weihrauch et al., 1999), or have higher basal ammonia levels in their interstitial fluids, so that an outwardly oriented ammonia gradient is maintained to enable excretion. In freshwater organisms, hemolymph/blood ammonia concentrations

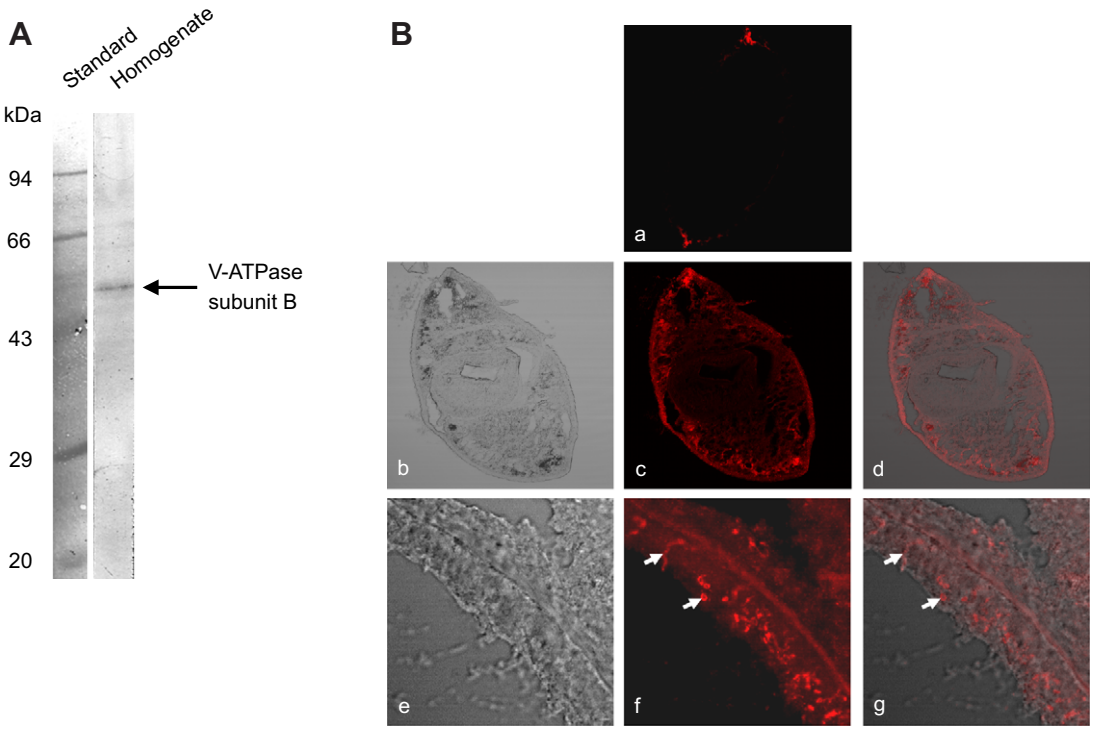

Fig. 7. Expression of V-ATPase subunit B in *S. mediterranea*. (A) Total protein extracts isolated from whole animals were probed with an antiserum raised against V-ATPase subunit B from *Manduca sexta*. A distinct band of approximately 56 kDa (calculated by migration distance), apparently V-ATPase subunit B, is detected, confirming expression of this subunit in *S. mediterranea*. (B) In cross-sections, the same antiserum detected a distinct signal in the epidermis of the animal that is mainly based on the staining of rod-shaped structures, presumably rhabdites (arrowheads). (a) Control without application of primary antibody; (b,e) brightfield; (a,c,f) fluorescence; (d) b and c merged; (g) e and f merged. Magnifications are: (a–d) ×100 and (e,f) ×400.

between ca. 0.1 and 0.5 mmol l^{-1} are very common. For instance, in the hemolymph of the freshwater crayfish *Cherax destructor* (Fellows and Hird, 1979) and the freshwater-acclimated Chinese mitten crab, *Eriocheir sinensis* (Weihrauch et al., 1999), values of ca. 100 and 116 μmol l^{-1} were measured. In freshwater trout (Zimmer et al., 2010), the mudpuppy *Necturus maculosus* and the fully aquatic *X. laevis* (Wood et al., 1989), blood ammonia concentrations of ca. 550, 150 and 116 μmol l^{-1}, respectively, were detected. In the present study, a 1 h exposure to ≥0.5 mmol l^{-1} NH_4Cl led to elevated post-exposure ammonia excretion rates, suggesting accumulation of ammonia within the body fluids during the treatment. It thus appears that ammonia excretion cannot counterbalance passive ammonia influxes at this level (Fig. 11).

Ammonia excretion mechanism

The ammonia excretion rate in *S. mediterranea* was highly influenced by the ambient pH (Fig. 4), suggesting an ammonia excretion mechanism based on ammonia trapping across the exposed body surface. Our data showed similar excretion rates in non-buffered water (pH 8.3) and in media strongly buffered to a pH between 5.5 and 6.5, indicating that the animal itself acidifies the unstirred boundary layer to that range of pH to promote ammonia excretion. This was also evident as a greatly reduced excretion rate when the environmental media was buffered to pH 8 and 8.5. Our attempts to measure the acidification and ammonia excretion on the body surface directly by employing the scanning ion-selective electrode technique (Donini and O'Donnell, 2005) failed because of the mucous layer that is excreted by the epidermis. Nevertheless, this mucous layer provides a microenvironment that most likely retains a low pH generated by the epidermis. The effects of inhibitors (Fig. 5) are also consistent with acidification of the apical unstirred boundary layer by the epidermis. Inhibitory effects of concanamycin C, amiloride and acetazolamide provide evidence of the involvement of a V-

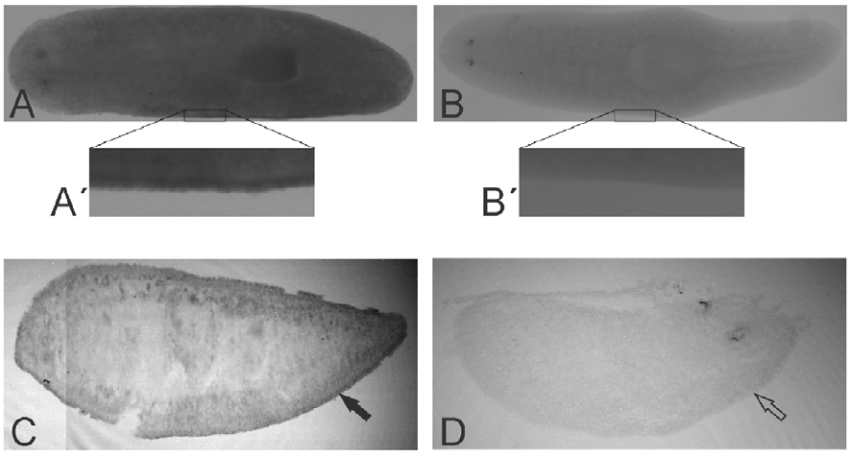

Fig. 8. Expression of Rh-like protein in *S. mediterranea*. In whole-mount preparations, application of antisense riboprobes specific to Rh-like protein mRNA resulted in a strong staining covering the complete animal (A). At higher magnifications, the strongest signal intensity was apparent at the periphery of the animals, presumably in the epidermis (A′). Application of sense probes did not elicit any signal (B,B′). In cross-sections, application of antisense riboprobes again resulted in a staining that resided mainly in the periphery of the animals, presumably epidermal cells (C, filled arrow), whereas sections incubated with sense probes did not show any staining (D, open arrow). Magnifications are: (A,B) ×30, (A′,B′) ×250 and (C,D) ×100.

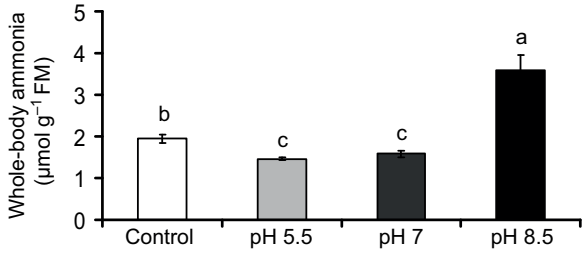

Fig. 9. Whole-body ammonia concentrations (means ± s.e.m.) in *S. mediterranea* after 48 h of exposure to control medium (dechlorinated tap water, pH 8.3; *N*=4) and media buffered to pH 5.5 (10 mmol l^{-1} MES; *N*=4), 7 (10 mmol l^{-1} HEPES; *N*=4) and 8.5 (10 mmol l^{-1} Tris; *N*=6). Significant differences are indicated by different letters. Data were analyzed employing a one-way ANOVA using a Tukey's pairwise comparison.

ATPase and a cation/proton exchanger in this process. Both transporters utilize protons provided by the activity of an intracellular carbonic anhydrase, a mechanism also suggested to function in the branchial pavement cells of freshwater fish (Nawata et al., 2007; Nawata and Wood, 2008; Nawata and Wood, 2009; Nawata et al., 2010b; Weihrauch et al., 2009).

Participation of an apically localized NHE, nhe3b, in ammonia excretion has most convincingly been shown in flux studies employing inhibitor experiments and nhe3b knockdown experiments in zebrafish larvae (Shih et al., 2012). The importance of an apical H^+-gradient in ammonia excretion is also evident by our data: even when acidification of the apical unstirred boundary layer by the V-ATPase, and/or possibly an NHE, was compromised because of the reduction of cytoplasmatic proton availability after inhibition of the carbonic anhydrase, an applied low apical pH enhanced the ammonia excretion rate to values well above control levels (Fig. 6). Although amiloride employed at higher concentrations blocks both NHEs and Na^+-channels (Kleyman and Cragoe, 1988) that might be present in the apical membrane of the epidermal epithelium, 2 mmol l^{-1} amiloride had no effect on ammonia excretion rates. This concentration is at least three orders of magnitudes higher than the IC_{50} reported for Na^+ channels (Kleyman and Cragoe, 1988), so an indirect inhibition of ammonia excretion as a result of a shift in membrane potential caused by a putative blockage of an apical Na^+ channel seems unlikely.

Although an NHE8-like cation/proton exchanger has been cloned in *S. mediterranea* (GenBank accession no. EG354491) and blockage of the ammonia excretion rate by high doses of amiloride does suggest the participation of an apical NHE, there is to date no proof for the presence of such a transporter in the apical membrane of the hypodermis. There is an open debate whether an electroneutral NHE that is driven only by the prevailing cation concentrations but not the electrical potential across the apical membrane could function in freshwater environments, as there is a potential threat of Na^+ loss (Orlowski and Grinstein, 2004; Parks et al., 2008). However, as mentioned above, there is recent evidence for the participation of an apically localized nhe3b in ammonia excretion in zebrafish larvae (Shih et al., 2012; Yan et al., 2007) and the presence of NHE2 and NHE3 in branchial Na^+/K^+-ATPase-positive peanut lectin agglutinin (PNA)-positive mitochondria-rich cells in rainbow trout (Ivanis et al., 2008). Moreover, there are precedents for electrogenic sodium:proton exchangers (i.e. 2 Na^+:1 H^+) in invertebrates (Ahearn et al., 2001) that are inhibited by amiloride and that would allow the influx of Na^+ to be driven in part by

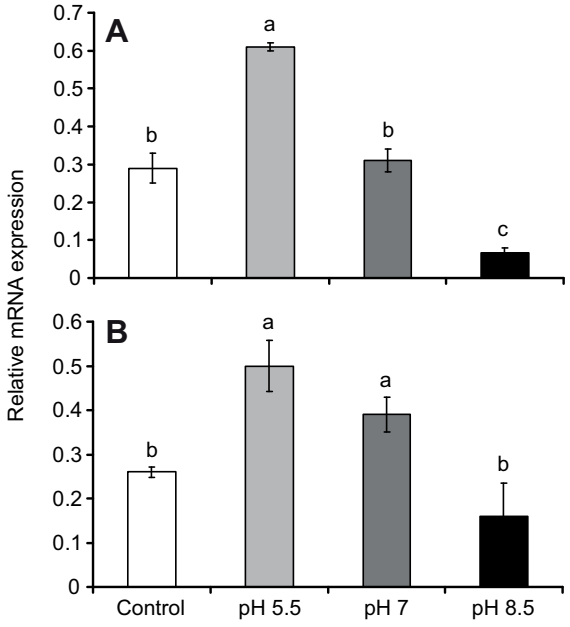

Fig. 10. Relative mRNA expression levels (means ± s.e.m.) of (A) Rh-like protein (*N*=4) and (B) V-ATPase (subunit A; *N*=4) in *S. mediterranea* under control conditions and after a 48 h exposure to media buffered to pH 5.5 (10 mmol l^{-1} MES), 7 (10 mmol l^{-1} HEPES) and 8.5 (10 mmol l^{-1} Tris). The ratio of absolute expression levels of the target genes and actin is shown. Significant differences are indicated by different letters. Data were analyzed employing a one-way ANOVA using a Tukey's pairwise comparison.

the transmembrane potential difference established by the electrogenic H^+-ATPase.

Clearly, more studies are necessary to evaluate the effects of amiloride on ammonia fluxes in *S. mediterranea*, including verification of the presence and the cellular localization of the NHE8-like or other NHE-like transporters in the hypodermis, as well as the characteristics of such transporters.

Employing an antibody raised against the subunit B of an invertebrate V-ATPase in cross-sections of *S. mediterranea*

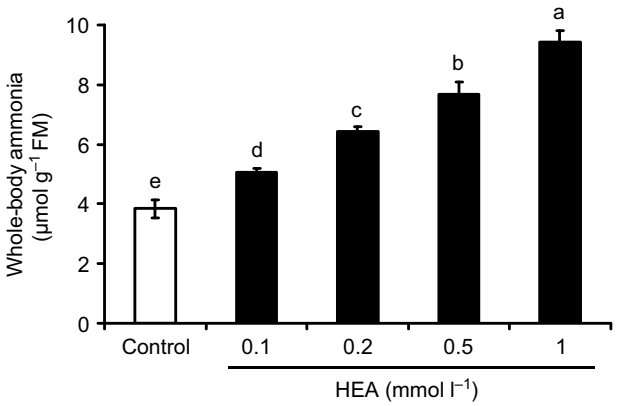

Fig. 11. Body ammonia concentrations (means ± s.e.m.) in *S. mediterranea* after 48 h exposure to control medium (dechlorinated tap water, pH 8.3) and different HEA concentrations (0.1, 0.2, 0.5 and 1 mmol l^{-1} NH_4Cl; *N*=5 for all treatments). Significant differences are indicated by different letters. Data were analyzed employing a one-way ANOVA using a Tukey's pairwise comparison.

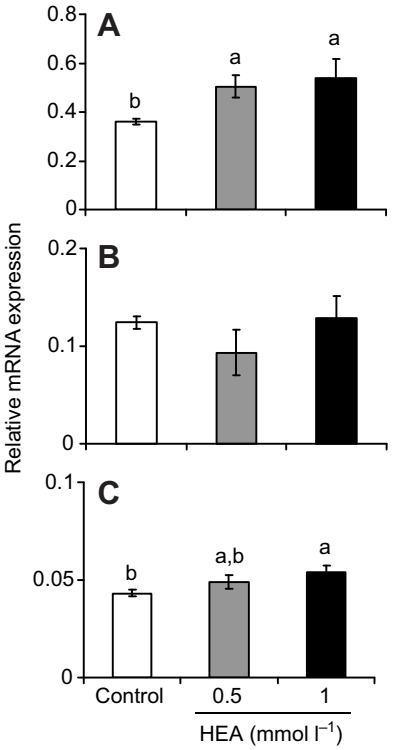

Fig. 12. Relative mRNA expression levels (means ± s.e.m.) of (A) Rh-like protein, (B) V-ATPase (subunit A) and (C) Na^+/K^+-ATPase (α-subunit) in *S. mediterranea* under control conditions and after a 48 h exposure to HEA (0.5 and 1 mmol l^{-1} NH_4Cl; N=4 for all treatments). The ratio of absolute expression levels of the target genes and actin is shown. Significant differences are indicated by different letters. Data were analyzed employing a one-way ANOVA using a Tukey's pairwise comparison.

confirmed abundance of the proton pump in the epidermis. The V-ATPase was particularly abundant in the rhabdites (Fig. 7), consistent with their acidophilic characteristics (Reisinger and Kelbetz, 1964; Stevenson and Beane, 2010). Although not shown explicitly in this study, an apical localization of the V-ATPase in the epidermal epithelium of *S. mediterranea* is plausible given widespread findings showing that proton pumps implicated in osmoregulatory NaCl uptake are localized to the apical surfaces in the skin and gills of freshwater organisms (Hwang, 2009; Klein et al., 1997; Lin et al., 2006; Onken and Putzenlechner, 1995; Patrick et al., 2006; Shih et al., 2008).

Apical exit of ammonia might be mediated by an Rh-like ammonia transporter that is highly expressed in the epidermis (Fig. 8), although it cannot be excluded that the identified Rh-like ammonia transporter is also or exclusively localized in the basolateral membrane and mediates hemolymph to cell ammonia uptake. Involvement of this protein in ammonia excretion is also implicated by changes in its mRNA expression level in response to changes in environmental pH, HEA and an internal ammonia load after feeding (Figs 2, 10, 12). In common with the teleost ammonia transporter Rhcg2, which is localized apically in the branchial pavement cells, the Rh-protein from *S. mediterranea* is upregulated during long-term HEA exposure. In contrast to Rhcg2, the basolateral ammonia transporter Rhbg is not influenced by HEA exposure in freshwater fish (Nawata et al., 2007). Considering its similar response (upregulation) to HEA exposure (Nawata et al., 2007; Zimmer et al., 2010) and feeding (Zimmer et al., 2010) (Figs 2, 12), we suggest that the Rh-protein in *S. mediterranea* is also apically expressed and that it functions in a fashion comparable to that of the branchial Rhcg2 from freshwater fish. A more detailed analysis of this transporter, including functional expression analysis and cellular localization studies, is clearly needed to justify this suggestion. An analysis of the published partial amino acid sequence of *S. mediterranea* (GenBank accession no. DN307511) revealed a high degree of identity to Rh-proteins with confirmed ammonia transport capacities, including amino acids that are critical for NH_3 conductance.

Basolateral entrance of extracellular ammonia into the cytoplasm of the ammonia-excreting epithelia is possibly mediated by the Na^+/K^+-ATPase, as evident by the ca. 50% reduction of excretion after inhibition of the pump (Fig. 5) and an mRNA upregulation of its α-subunit after HEA exposure (Fig. 12). Comparatively high concentrations (1 mmol l^{-1}) of ouabain were required to obtain an inhibitory effect, as this pump is most likely inserted in the basolateral membrane and can thereby not be targeted directly.

In both vertebrate and invertebrate systems, the Na^+/K^+-ATPase accepts NH_4^+ ions as a substrate, thereby facilitating the active transport of extracellular NH_4^+ into the epithelial cell (Furriel et al., 2004; Kurtz and Balaban, 1986; Mallery, 1983; Masui et al., 2002; Nawata et al., 2010a; Skou, 1960; Wall and Koger, 1994). Blockage of the Na^+/K^+-ATPase may also inhibit ammonia excretion indirectly because of a reduced 'out-to-in' Na^+ gradient and a consequent reduction in apical acidification *via* NHE if present.

An intracellular vesicular transport of NH_4^+, as proposed for the branchial ammonia transport in *C. maenas* (Weihrauch et al., 2002) or in the midgut of *M. sexta* (Weihrauch, 2006) is unlikely, as application of a high concentration of the microtubule blocker colchicine showed no inhibitory effect on ammonia excretion by *S. mediterranea*. Responses of ammonia excretion rates measured after manipulations of the environmental media in short-term experiments suggests that a portion, if not the majority, of metabolic ammonia is indeed excreted *via* the body surface and not *via* the protonephridia because these short-term treatments would likely not have affected the internal excretory tissues. Moreover, the Rh-protein and V-ATPase, transporters involved in the ammonia excretory process, were found in high abundance in the epidermis (Figs 7, 8). A hypothetical working model of the ammonia excretion mechanism suggested in the epidermal epithelium is summarized in Fig. 13.

The effect of long-term exposure to varying pH regimes

Long-term exposure to varying environmental pH regimes caused changes in whole-body ammonia levels and mRNA expression levels of the Rh-protein and V-ATPase, but had no effect on whole-body pH. A 2 day exposure to an environmental pH of 5.5 caused a slight decrease in body ammonia concentration, likely because of the body-to-environment ΔP_{NH_3} (~50-fold outwardly directed NH_3 gradient) at this pH regime that favours NH_3 excretion. The relatively high mRNA expression level of Rh-protein observed after the exposure would promote NH_3 excretion. Moreover, it has been suggested that Rh-proteins also promote the transport of CO_2 (Musa-Aziz et al., 2009; Perry et al., 2010; Soupene et al., 2004). One could therefore further speculate that this high abundance of the Rh-protein in the epidermis promotes excretion of metabolic CO_2 in planarians stressed by low pH. In parallel, expression of the V-ATPase (subunit A) is also elevated, possibly to counteract the inward proton gradient and to maintain pH homeostasis.

As observed in trout embryos (Sashaw et al., 2010), exposure to a high environmental pH caused an accumulation of body ammonia

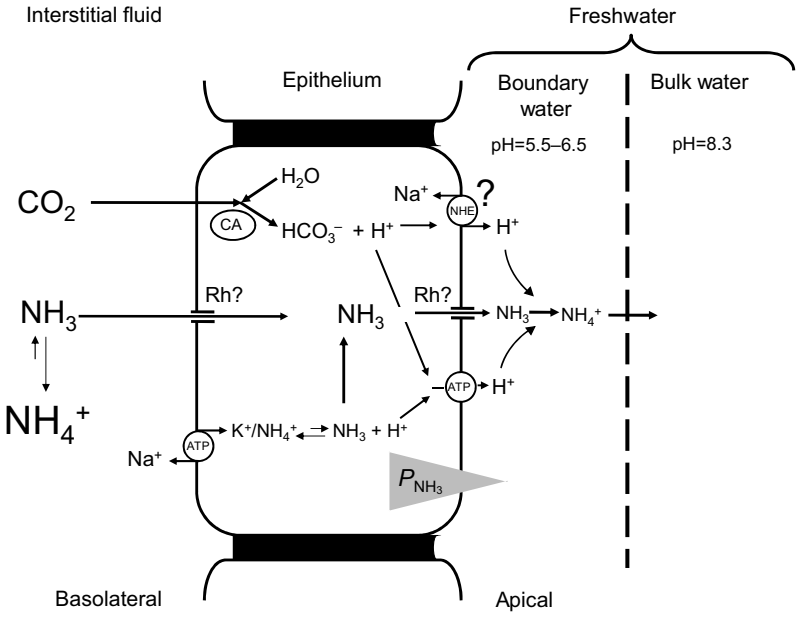

Fig. 13. Proposed hypothetical model of ammonia excretion across the epidermal epithelium in the freshwater planarian *S. mediterranea*. Hemolymph NH_4^+ is pumped across the basolateral membrane by the Na^+/K^+-ATPase into the cytoplasm or enters as NH_3 *via* an Rh-like ammonia transporter. Protons generated by a cytoplasmatic carbonic anhydrase (CA) are transported *via* an apical V-ATPase and possibly also *via* a cation/proton exchanger (NHE) across the apical membrane, acidifying the unstirred boundary layer to a pH of approximately 5.5–6.5. The low pH traps NH_3 as NH_4^+ as it passively diffuses into the unstirred boundary water along the maintained transcellular P_{NH_3} gradient. It is proposed that an identified Rh-like ammonia transporter mediates this apical NH_3 transport. Transport characteristics and basolateral *versus* apical localization of the planarian ammonia transporter (Rh-protein) are presently unknown (indicated by '?'). The model assumes that paracellular NH_4^+ diffusion is negligible, given that in freshwater organisms, epithelia facing the environment generally show a very low ion conductance to avoid passive effluxes along a steep osmotic gradient (Civan et al., 1985; Weber et al., 1995; Weihrauch et al., 1999).

levels in *S. mediterranea* (Fig. 9), likely because of a hampered ammonia excretion at these unfavourable conditions (see Fig. 4). The corresponding downregulation of the Rh-protein in *S. mediterranea* may serve as a protective mechanism to reduce the entrance of environmental NH_3 or the exit of metabolic CO_2, the latter in order to retain acid equivalents. In parallel to the Rh-protein, the V-ATPase, which is also found in high abundance in the epidermis (Fig. 7), showed a trend towards downregulation relative to expression levels in animals exposed to pH 5.5 and 7 (Fig. 10). Such a downregulation would reduce active H^+ loss into a medium that cannot be acidified owing to not only its artificial high buffer capacity but also its energy consumption.

The effect of long term exposure to HEA

The whole-body ammonia concentrations in *S. mediterranea* (1.9±0.1 μmol g^{-1} FM) were similar to values measured in the freshwater ribbon leech *Nephelopsis obscura* (D.W., unpublished), but well above of those reported for trout embryos (ca. 0.25 μmol g^{-1} FM) (Sashaw et al., 2010). Tolerance to high body ammonia and the capability for an active or secondary active ammonia excretion mode might be attributable to the benthic lifestyle of many freshwater planarians (Lombardo et al., 2011). Long-term exposure even to low environmental ammonia concentrations (100 μmol l^{-1} NH_4Cl) caused an increase in body ammonia levels, suggesting that normal ammonia concentrations in the interstitial fluids are fairly low.

In *S. mediterranea*, relative mRNA expression levels of the Rh-like protein were upregulated after exposure to HEA (Fig. 12), a phenomenon also observed for the apical localized Rhcg2 in embryonic and adult trout (Nawata et al., 2007; Sashaw et al., 2010) and branchial Rh-protein expression of a marine decapod crab (Martin et al., 2011). However, in contrast to trout (Nawata et al., 2007; Sashaw et al., 2010) and marine *Metacarcinus magister* crabs (Martin et al., 2011), the V-ATPase was not upregulated after a 2 day HEA exposure, a puzzling finding because this pump, as discussed above, is most likely a key player in the ammonia excretion mechanism in *S. mediterranea*. A detailed analysis of the influence of HEA exposure on epidermal gene expression may provide further insight into the role that this pump holds in ammonia excretion. The observed upregulation of the Na^+/K^+-ATPase after HEA exposure implies that this pump plays a significant role in ammonia homeostasis under challenging conditions.

Conclusions

This study provides the first comprehensive investigation of ammonia excretion mechanisms in a freshwater invertebrate species. Our findings suggest that the machinery that is involved in epidermal ammonia excretion in a planarian species is very similar to the excretion mechanism proposed to be functioning in the gills of freshwater fish. This mode of excretion may be quite common and may have evolved fairly early, prior to the appearance of vertebrates. *Schmidtea mediterranea* is amenable to a wide range of molecular techniques and will be of future use in determining the mechanisms of ammonia excretion at the molecular level.

ACKNOWLEDGEMENTS

We thank Dr Helmut Wieczorek for providing the anti V-ATPase subunit B antiserum. The authors would like to thank the reviewers for their constructive comments in the review of this manuscript.

FUNDING

This work was supported by Natural Sciences and Engineering Research Council Canada Discovery Grants to D.W. and M.J.O., and by the German Research Foundation to H.M. (SFB 944: Physiology and dynamics of cellular microcompartments).

REFERENCES

Ahearn, G. A., Mandal, P. K. and Mandal, A. (2001). Biology of the $2Na^+/1H^+$ antiporter in invertebrates. *J. Exp. Zool.* **289**, 232-244.

Blaesse, A. K., Broehan, G., Meyer, H., Merzendorfer, H. and Weihrauch, D. (2010). Ammonia uptake in *Manduca sexta* midgut is mediated by an amiloride sensitive cation/proton exchanger: Transport studies and mRNA expression analysis of NHE7, 9, NHE8, and V-ATPase (subunit D). *Comp. Biochem. Physiol.* **157A**, 364-376.

Braun, M. H., Steele, S. L., Ekker, M. and Perry, S. F. (2009). Nitrogen excretion in developing zebrafish (*Danio rerio*): a role for Rh proteins and urea transporters. *Am. J. Physiol.* **296**, F994-F1005.

Butterworth, R. F. (2002). Pathophysiology of hepatic encephalopathy: a new look at ammonia. *Metab. Brain Dis.* **17**, 221-227.

Cameron, J. N. and Heisler, N. (1983). Studies of ammonia in the rainbow trout: physicochemical parameters, acid-base behaviour and respiratory clearance. *J. Exp. Biol.* **105**, 107-125.

Chan, H., Hazell, A. S., Desjardins, P. and Butterworth, R. F. (2000). Effects of ammonia on glutamate transporter (GLAST) protein and mRNA in cultured rat cortical astrocytes. *Neurochem. Int.* **37**, 243-248.

Chintapalli, V. R., Wang, J. and Dow, J. A. (2007). Using FlyAtlas to identify better *Drosophila melanogaster* models of human disease. *Nat. Genet.* **39**, 715-720.
Civan, M. M., Rubenstein, D., Mauro, T. and O'Brien, T. G. (1985). Effects of tumor promoters on sodium ion transport across frog skin. *Am. J. Physiol.* **248**, C457-C465.
Cragg, M. M., Balinsky, J. B. and Baldwin, E. (1961). A comparative study of nitrogen excretion in some Amphibia and reptiles. *Comp. Biochem. Physiol.* **3**, 227-235.
Donini, A. and O'Donnell, M. J. (2005). Analysis of Na^+, Cl^-, K^+, H^+ and NH_4^+ concentration gradients adjacent to the surface of anal papillae of the mosquito *Aedes aegypti*: application of self-referencing ion-selective microelectrodes. *J. Exp. Biol.* **208**, 603-610.
Downie, J. A., Gibson, F. and Cox, G. B. (1979). Membrane adenosine triphosphatases of prokaryotic cells. *Annu. Rev. Biochem.* **48**, 103-131.
Fanelli, G. M. and Goldstein, L. (1964). Ammonia excretion in the neotenous newt, *Necturus maculosus* (Rafinesque). *Comp. Biochem. Physiol.* **13**, 193-204.
Fellows, F. C. I. and Hird, F. J. R. (1979). Nitrogen metabolism and excretion in the freshwater crayfish *Cherax destructor*. *Comp. Biochem. Physiol.* **64B**, 235-238.
Furriel, R. P., Masui, D. C., McNamara, J. C. and Leone, F. A. (2004). Modulation of gill Na^+,K^+-ATPase activity by ammonium ions: putative coupling of nitrogen excretion and ion uptake in the freshwater shrimp *Macrobrachium olfersii*. *J. Exp. Zool. A* **301**, 63-74.
Hwang, P. P. (2009). Ion uptake and acid secretion in zebrafish (*Danio rerio*). *J. Exp. Biol.* **212**, 1745-1752.
Ip, Y. K. and Chew, S. F. (2010). Ammonia production, excretion, toxicity and defense in fish: a review. *Front. Physiol.* **1**, 1-20.
Ivanis, G., Esbaugh, A. J. and Perry, S. F. (2008). Branchial expression and localization of SLC9A2 and SLC9A3 sodium/hydrogen exchangers and their possible role in acid–base regulation in freshwater rainbow trout (*Oncorhynchus mykiss*). *J. Exp. Biol.* **211**, 2467-2477.
Klein, U., Timme, M., Zeiske, W. and Ehrenfeld, J. (1997). The H^+ pump in frog skin (*Rana esculenta*): identification and localization of a V-ATPase. *J. Membr. Biol.* **157**, 117-126.
Kleyman, T. R. and Cragoe, E. J., Jr (1988). Amiloride and its analogs as tools in the study of ion transport. *J. Membr. Biol.* **105**, 1-21.
Knecht, K., Michalak, A., Rose, C., Rothstein, J. D. and Butterworth, R. F. (1997). Decreased glutamate transporter (GLT-1) expression in frontal cortex of rats with acute liver failure. *Neurosci. Lett.* **229**, 201-203.
Kurtz, I. and Balaban, R. S. (1986). Ammonium as a substrate for Na^+-K^+-ATPase in rabbit proximal tubules. *Am. J. Physiol.* **250**, F497-F502.
Lin, L. Y., Horng, J. L., Kunkel, J. G. and Hwang, P. P. (2006). Proton pump-rich cell secretes acid in skin of zebrafish larvae. *Am. J. Physiol.* **290**, C371-C378.
Lombardo, P., Giustini, M., Miccoli, F. P. and Cicolani, B. (2011). Fine-scale differences in diel activity among nocturnal freshwater planarias (Platyhelminthes: Tricladida). *J. Circadian Rhythms* **9**, 2.
Lucu, C., Devescovi, M. and Siebers, D. (1989). Do amiloride and ouabain affect ammonia fluxes in perfused *Carcinus* gill epithelia? *J. Exp. Zool.* **249**, 1-5.
Mallery, C. H. (1983). A carrier enzyme basis for ammonium excretion in teleost gill. NH^+_4-stimulated Na-dependent ATPase activity in *Opsanus beta*. *Comp. Biochem. Physiol.* **74A**, 889-897.
Marcaida, G., Felipo, V., Hermenegildo, C., Miñana, M. D. and Grisolía, S. (1992). Acute ammonia toxicity is mediated by the NMDA type of glutamate receptors. *FEBS Lett.* **296**, 67-68.
Marini, A.-M., Matassi, G., Raynal, V., André, B., Cartron, J.-P. and Chérif-Zahar, B. (2000). The human Rhesus-associated RhAG protein and a kidney homologue promote ammonium transport in yeast. *Nat. Genet.* **26**, 341-344.
Martin, M., Fehsenfeld, S., Sourial, M. M. and Weihrauch, D. (2011). Effects of high environmental ammonia on branchial ammonia excretion rates and tissue Rh-protein mRNA expression levels in seawater acclimated Dungeness crab *Metacarcinus magister*. *Comp. Biochem. Physiol.* **160A**, 267-277.
Masui, D. C., Furriel, R. P., McNamara, J. C., Mantelatto, F. L. and Leone, F. A. (2002). Modulation by ammonium ions of gill microsomal (Na+,K+)-ATPase in the swimming crab Callinectes danae: a possible mechanism for regulation of ammonia excretion. *Comp. Biochem. Physiol.* **132C**, 471-482.
Merzendorfer, H., Gräf, R., Huss, M., Harvey, W. R. and Wieczorek, H. (1997). Regulation of proton-translocating V-ATPases. *J. Exp. Biol.* **200**, 225-235.
Meyer, H., Panz, M., Zmojdzian, M., Jagla, K. and Paululat, A. (2009). Neprilysin 4, a novel endopeptidase from *Drosophila melanogaster*, displays distinct substrate specificities and exceptional solubility states. *J. Exp. Biol.* **212**, 3673-3683.
Musa-Aziz, R., Chen, L. M., Pelletier, M. F. and Boron, W. F. (2009). Relative CO_2/NH_3 selectivities of AQP1, AQP4, AQP5, AmtB, and RhAG. *Proc. Natl. Acad. Sci. USA* **106**, 5406-5411.
Nawata, C. M., Hung, C. C., Tsui, T. K., Wilson, J. M., Wright, P. A. and Wood, C. M. (2007). Ammonia excretion in rainbow trout (*Oncorhynchus mykiss*): evidence for Rh glycoprotein and H^+-ATPase involvement. *Physiol. Genomics* **31**, 463-474.
Nawata, C. M. and Wood, C. M. (2008). The effects of CO2 and external buffering on ammonia excretion and Rhesus glycoprotein mRNA expression in rainbow trout. *J. Exp. Biol.* **211**, 3226-3236.
Nawata, C. M. and Wood, C. M. (2009). mRNA expression analysis of the physiological responses to ammonia infusion in rainbow trout. *J. Comp. Physiol. B* **179**, 799-810.
Nawata, C. M., Hirose, S., Nakada, T., Wood, C. M. and Kato, A. (2010a). Rh glycoprotein expression is modulated in pufferfish (*Takifugu rubripes*) during high environmental ammonia exposure. *J. Exp. Biol.* **213**, 3150-3160.
Nawata, C. M., Wood, C. M. and O'Donnell, M. J. (2010b). Functional characterization of Rhesus glycoproteins from an ammoniotelic teleost, the rainbow trout, using oocyte expression and SIET analysis. *J. Exp. Biol.* **213**, 1049-1059.
Nogi, T. and Levin, M. (2005). Characterization of innexin gene expression and functional roles of gap-junctional communication in planarian regeneration. *Dev. Biol.* **287**, 314-335.
Norenberg, M. D., Huo, Z., Neary, J. T. and Roig-Cantesano, A. (1997). The glial glutamate transporter in hyperammonemia and hepatic encephalopathy: relation to energy metabolism and glutamatergic neurotransmission. *Glia* **21**, 124-133.
Onken, H. and McNamara, J. C. (2002). Hyperosmoregulation in the red freshwater crab *Dilocarcinus pagei* (Brachyura, Trichodactylidae): structural and functional asymmetries of the posterior gills. *J. Exp. Biol.* **205**, 167-175.
Onken, H. and Putzenlechner, M. (1995). A V-ATPase drives active, electrogenic and Na^+-independent Cl^- absorption across the gills of *Eriocheir sinensis*. *J. Exp. Biol.* **198**, 767-774.
Orlowski, J. and Grinstein, S. (2004). Diversity of the mammalian sodium/proton exchanger SLC9 gene family. *Pflugers Arch.* **447**, 549-565.
Parks, S. K., Tresguerres, M. and Goss, G. G. (2008). Theoretical considerations underlying Na^+ uptake mechanisms in freshwater fishes. *Comp. Biochem. Physiol.* **148C**, 411-418.
Patrick, M. L., Aimanova, K., Sanders, H. R. and Gill, S. S. (2006). P-type Na^+/K^+-ATPase and V-type H^+-ATPase expression patterns in the osmoregulatory organs of larval and adult mosquito *Aedes aegypti*. *J. Exp. Biol.* **209**, 4638-4651.
Perry, S. F., Braun, M. H., Noland, M., Dawdy, J. and Walsh, P. J. (2010). Do zebrafish Rh proteins act as dual ammonia-CO_2 channels? *J. Exp. Zool. A* **313**, 618-21.
Potts, W. T. (1965). Ammonia excretion in *Octopus dofleini*. *Comp. Biochem. Physiol.* **14**, 339-355.
Reisinger, E. and Kelbetz, S. (1964). Fine structure and discharge mechanism of rhabdites. *Z. Wiss. Mikrosk.* **65**, 472-508.
Rompolas, P., Patel-King, R. S. and King, S. M. (2009). Schmidtea mediterranea: a model system for analysis of motile cilia. *Methods Cell Biol.* **93**, 81-98.
Sánchez Alvarado, A. and Newmark, P. A. (1999). Double-stranded RNA specifically disrupts gene expression during planarian regeneration. *Proc. Natl. Acad. Sci. USA* **96**, 5049-5054.
Sánchez Alvarado, A. and Tsonis, P. A. (2006). Bridging the regeneration gap: genetic insights from diverse animal models. *Nat. Rev. Genet.* **7**, 873-884.
Sashaw, J., Nawata, M., Thompson, S., Wood, C. M. and Wright, P. A. (2010). Rhesus glycoprotein and urea transporter genes in rainbow trout embryos are upregulated in response to alkaline water (pH 9.7) but not elevated water ammonia. *Aquat. Toxicol.* **96**, 308-313.
Shih, T. H., Horng, J. L., Hwang, P. P. and Lin, L. Y. (2008). Ammonia excretion by the skin of zebrafish (*Danio rerio*) larvae. *Am. J. Physiol.* **295**, C1625-C1632.
Shih, T. H., Horng, J. L., Liu, S. T., Hwang, P. P. and Lin, L. Y. (2012). Rhcg1 and NHE3b are involved in ammonium-dependent sodium uptake by zebrafish larvae acclimated to low-sodium water. *Am. J. Physiol.* **302**, R84-R93.
Skou, J. C. (1960). Further investigations on a Mg^{++} + Na^+-activated adenosine triphosphatase, possibly related to the active, linked transport of Na^+ and K^+ across the nerve membrane. *Biochim. Biophys. Acta* **42**, 6-23.
Soupene, E., Inwood, W. and Kustu, S. (2004). Lack of the Rhesus protein Rh1 impairs growth of the green alga *Chlamydomonas reinhardtii* at high CO_2. *Proc. Natl. Acad. Sci. USA* **101**, 7787-7792.
Stevenson, C. G. and Beane, W. S. (2010). A low percent ethanol method for immobilizing planarians. *PLoS ONE* **5**, e15310.
Umesono, Y., Watanabe, K. and Agata, K. (1999). Distinct structural domains in the planarian brain defined by the expression of evolutionarily conserved homeobox genes. *Dev. Genes Evol.* **209**, 31-39.
Wall, S. M. and Koger, L. M. (1994). NH^+_4 transport mediated by Na^+-K^+-ATPase in rat inner medullary collecting duct. *Am. J. Physiol.* **267**, F660-F670.
Weber, W. M., Liebold, K. M. and Clauss, W. (1995). Amiloride-sensitive Na^+ conductance in native *Xenopus* oocytes. *Biochim. Biophys. Acta* **1239**, 201-206.
Weihrauch, D. (1999). *Zur Stickstoff-Exkretion aquatischer Brachyuren:* Carcinus maenas *(Linnaeus 1758, Decapoda, Portunidae),* Cancer pagurus *Linnaeus 1758 (Decapoda, Cancridae) und* Eriocheir sinensis *H. Milne Edwards 1853 (Decapoda, Grapsidae)*. Berlin: VWF Verlag fuer Wissenschaft und Forschung.
Weihrauch, D. (2006). Active ammonia absorption in the midgut of the tobacco hornworm *Manduca sexta* L.: transport studies and mRNA expression analysis of a Rhesus-like ammonia transporter. *Insect Biochem. Mol. Biol.* **36**, 808-821.
Weihrauch, D., Becker, W., Postel, U., Riestenpatt, S. and Siebers, D. (1998). Active excretion of ammonia across the gills of the shore crab *Carcinus maenas* and its relation to osmoregulatory ion uptake. *J. Comp. Physiol. B* **168**, 364-376.
Weihrauch, D., Becker, W., Postel, U., Luck-Kopp, S. and Siebers, D. (1999). Potential of active excretion of ammonia in three different haline species of crabs. *J. Comp. Physiol. B* **169**, 25-37.
Weihrauch, D., Ziegler, A., Siebers, D. and Towle, D. W. (2001). Molecular characterization of V-type H^+-ATPase (B-subunit) in gills of euryhaline crabs and its physiological role in osmoregulatory ion uptake. *J. Exp. Biol.* **204**, 25-37.
Weihrauch, D., Ziegler, A., Siebers, D. and Towle, D. W. (2002). Active ammonia excretion across the gills of the green shore crab *Carcinus maenas*: participation of Na^+/K^+-ATPase, V-type H^+-ATPase and functional microtubules. *J. Exp. Biol.* **205**, 2765-2775.
Weihrauch, D., McNamara, J. C., Towle, D. W. and Onken, H. (2004a). Ion-motive ATPases and active, transbranchial NaCl uptake in the red freshwater crab, *Dilocarcinus pagei* (Decapoda, Trichodactylidae). *J. Exp. Biol.* **207**, 4623-4631.
Weihrauch, D., Morris, S. and Towle, D. W. (2004b). Ammonia excretion in aquatic and terrestrial crabs. *J. Exp. Biol.* **207**, 4491-4504.
Weihrauch, D., Wilkie, M. P. and Walsh, P. J. (2009). Ammonia and urea transporters in gills of fish and aquatic crustaceans. *J. Exp. Biol.* **212**, 2879.
Weng, X. H., Huss, M., Wieczorek, H. and Beyenbach, K. W. (2003). The V-type H^+-ATPase in Malpighian tubules of *Aedes aegypti*: localization and activity. *J. Exp. Biol.* **206**, 2211-2219.
Wildling, S. and Kerschbaum, H. H. (2007). Nitric oxide decreases ammonium release in tadpoles of the clawed frog, *Xenopus laevis*, Daudin. *J. Comp. Physiol. B* **177**, 401-411.

Wilson, R., Wright, P., Munger, S. and Wood, C. (1994). Ammonia excretion in freshwater rainbow trout (*Oncorhynchus mykiss*) and the importance of gill boundary layer acidification: lack of evidence for Na^+/NH_4^+ exchange. *J. Exp. Biol.* **191**, 37-58.

Wood, C. M., Munger, R. S. and Toews, D. P. (1989). Ammonia, urea and H^+ distribution and the evolution of ureotelism in amphibians. *J. Exp. Biol.* **144**, 215-233.

Wright, P. A. (1995). Nitrogen excretion: three end products, many physiological roles. *J. Exp. Biol.* **198**, 273-281.

Wright, P. A. and Wood, C. M. (2009). A new paradigm for ammonia excretion in aquatic animals: role of Rhesus (Rh) glycoproteins. *J. Exp. Biol.* **212**, 2303-2312.

Yan, J. J., Chou, M. Y., Kaneko, T. and Hwang, P. P. (2007). Gene expression of Na^+/H^+ exchanger in zebrafish H^+-ATPase-rich cells during acclimation to low-Na^+ and acidic environments. *Am. J. Physiol.* **293**, C1814-C1823.

Zimmer, A. M., Nawata, C. M. and Wood, C. M. (2010). Physiological and molecular analysis of the interactive effects of feeding and high environmental ammonia on branchial ammonia excretion and Na^+ uptake in freshwater rainbow trout. *J. Comp. Physiol. B* **180**, 1191-1204.